

# THz photomixing synthesizer based on a fiber frequency comb

Gaël Mouret<sup>1\*</sup>, Francis Hindle<sup>1</sup>, Arnaud Cuisset<sup>1</sup>, Chun Yang<sup>1</sup>, Robin Bocquet<sup>1</sup>, Michel Lours<sup>2</sup>, and Daniele Rovera<sup>2</sup>

<sup>1</sup>Université du Littoral Côte d'Opale, Laboratoire de Physico Chimie de l'Atmosphère  
UMR CNRS 8101, 189 A Avenue Maurice Schumann, 59140 Dunkerque, France

<sup>2</sup>Observatoire de Paris, Systèmes de Référence Temps-Espace UMR CNRS 8630,  
61 avenue de l'Observatoire, 75014 Paris, France

\*mouret@univ-littoral.fr

**Abstract:** A frequency doubled erbium doped modelocked fiber frequency comb is used to implement a THz photomixing synthesizer. The useful THz linewidth is in order of 150 kHz and has been assessed along with the frequency accuracy by spectroscopic measurements demonstrating a relative accuracy of  $10^{-8}$  at frequencies around 1 THz. The THz synthesizer is used to implement a THz spectrometer to study the rotational absorption spectrum of carbonyl sulfide (OCS). Measurement of the principal transitions between 813 GHz and 1283 GHz allowed the properties of the THz spectrometer to be compared with competing techniques, and demonstrates the potential of the THz photomixing synthesizer as an alternative means to explore the THz domain.

©2009 Optical Society of America

**OCIS codes:** (120.0120) Instrumentation, measurement, and metrology; (120.3930) Metrological instrumentation; (300.6495) Spectroscopy, terahertz.

---

## References and links

1. D. M. Mittleman, *Sensing with THz radiation* (Springer, 2003).
2. E. R. Brown, K. A. McIntosh, K. B. Nichols, and C. L. Dennis, "Photomixing up to 3.8 THz in low-temperature-grown GaAs," *Appl. Phys. Lett.* **66**(3), 285–287 (1995).
3. C. Yang, J. Buldyreva, I. Gordon, F. Rohart, A. Cuisset, G. Mouret, R. Bocquet, and F. Hindle, "Oxygen, nitrogen and air broadening of HCN spectral lines at terahertz frequencies," *J. Quant. Spectrosc. Radiat. Transf.* **109**(17-18), 2857–2868 (2008).
4. I. Park, C. Sydlo, I. Fischer, W. Elsässer, and H. L. Hartnagel, "Generation and spectroscopic application of tunable continuous-wave terahertz radiation using a dual-mode semiconductor laser," *Meas. Sci. Technol.* **19**(6), 065305 (2008).
5. F. Hindle, A. Cuisset, R. Bocquet, and G. Mouret, "Continuous -wave THz by photomixing: application to gas pollutant detection and quantification," *Compte rendu de l'Académie des Sciences* **9**, 262–275 (2008).
6. S. Matsuura, M. Tani, H. Abe, K. Sakai, H. Ozeki, and S. Saito, "High-Resolution Terahertz Spectroscopy by a Compact Radiation Source Based on Photomixing with Diode Lasers in a Photoconductive Antenna," *J. Mol. Spectrosc.* **187**(1), 97–101 (1998).
7. A. S. Pine, R. D. Suenram, E. R. Brown, and K. A. McIntosh, "A Terahertz Photomixing Spectrometer: Application to SO<sub>2</sub> Self Broadening," *J. Mol. Spectrosc.* **175**(1), 37–47 (1996).
8. S. Matton, F. Rohart, R. Bocquet, D. Bigourd, A. Cuisset, F. Hindle, and G. Mouret, "Terahertz spectroscopy applied to the measurement of strengths and self-broadening coefficients for high-J lines of OCS," *J. Mol. Spectrosc.* **239**(2), 182–189 (2006).
9. S. Matsuura, P. Chen, G. A. Blake, and H. M. Pickett, "A tunable cavity-locked diode laser source for terahertz photomixing," *IEEE Trans. Microw. Theory Tech.* **48**(3), 380–387 (2000).
10. P. Chen, J. C. Pearson, H. M. Pickett, S. Matsuura, and G. A. Blake, "Submillimeter-wave measurements and analysis of the ground and  $v(2)=1$  states of water," *Astrophys. J. Suppl. Ser.* **128**(1), 371–385 (2000).
11. P. Chen, J. C. Pearson, H. M. Pickett, S. Matsuura, and G. A. Blake, "Measurements of 14NH<sub>3</sub> in the  $v_2=1$  state by a solid-state, photomixing, THz spectrometer, and a simultaneous analysis of the microwave, terahertz, and infrared transitions between the ground and  $v_2$  inversion–rotation levels," *J. Mol. Spectrosc.* **236**(1), 116–126 (2006).
12. L. Aballea, and L. F. Constantin, "Optoelectronic difference-frequency synthesizer: terahertz-waves for high-resolution spectroscopy," *Eur. Phys. J. Appl. Phys.* **45**(2), 21201 (2009).
13. S. T. Cundiff, and L. Hollberg, "Absolute Optical Frequency Metrology", *Encyclopedia of Modern Optics*, 82–90 (2004).
14. T. W. Hänsch, "Nobel Lecture: Passion for precision," *Rev. Mod. Phys.* **78**(4), 1297–1309 (2006).

15. J. L. Hall, "Nobel Lecture: Defining and measuring optical frequencies," *Rev. Mod. Phys.* **78**(4), 1279–1295 (2006).
16. Q. Quraishi, M. Griebel, T. Kleine-Ostmann, and R. Bratschitsch, "Generation of phase-locked and tunable continuous-wave radiation in the terahertz regime," *Opt. Lett.* **30**(23), 3231–3233 (2005).
17. J. J. McFerran, W. C. Swann, B. R. Washburn, and N. R. Newbury, "Elimination of pump-induced frequency jitter on fiber-laser frequency combs," *Opt. Lett.* **31**(13), 1997–1999 (2006).
18. A. Fayt, R. Vandenhoute, and J. G. Lahaye, "Global rovibrational analysis of carbonyl sulfide," *J. Mol. Spectrosc.* **119**(2), 233–266 (1986).
19. H. M. Pickett, R. L. Poynter, E. A. Cohen, M. L. Delitsky, J. C. Pearson, and H. S. P. Muller, "Submillimeter, Millimeter, and Microwave Spectral Line Catalog," *J. Quant. Spectrosc. Radiat. Transf.* **60**(5), 883–890 (1998).
20. P. Helminger, F. C. De Lucia, and W. Gordy, "Extension of microwave absorption spectroscopy to 0.37–mm wavelength," *Phys. Rev. Lett.* **25**(20), 1397–1399 (1970).
21. G. Y. Golubiatnikov, A. V. Lapinov, A. Guarnieri, and R. Knöchel, "Precise Lamb-dip measurements of millimeter and submillimeter wave rotational transitions of  $^{16}\text{O}^{12}\text{C}^{32}\text{S}$ ," *J. Mol. Spectrosc.* **234**(1), 190–194 (2005).
22. H. M. Pickett, "The fitting and predictions of vibration-rotation spectra with spin interactions," *J. Mol. Spectrosc.* **148**(2), 371–377 (1991).
23. D. L. Albritton, A. L. Schmeltekopf, and R. N. Zare, "An introduction to the Least-Squares Fitting of Spectroscopic Data", in *Molecular Spectroscopy: Modern Research*, K.N. Rao, ed. (Academic Press, New York, 1976).
24. D. Bigourd, A. Cuisset, F. Hindle, S. Matton, R. Bocquet, G. Mouret, F. Cazier, D. Dewaele, and H. Nouali, "Multiple component analysis of cigarette smoke using THz spectroscopy. Comparison with standard chemical analytical methods," *Appl. Phys. B* **86**(4), 579–586 (2007).
25. D. Bigourd, A. Cuisset, F. Hindle, S. Matton, E. Fertein, R. Bocquet, and G. Mouret, "Detection and quantification of multiple molecular species in mainstream cigarette smoke by continuous-wave terahertz spectroscopy," *Opt. Lett.* **31**(15), 2356–2358 (2006).
26. H. Ito, F. Nakajima, T. Furuta, and T. Ishibashi, "Continuous THz-wave generation using antenna-integrated uni-travelling-carrier photodiodes," *Semicond. Sci. Technol.* **20**(7), S191–S198 (2005).
27. A. Beck, G. Ducournau, M. Zaknune, E. Peytavit, T. Akalin, J. F. Lampin, F. Mollot, F. Hindle, C. Yang, and G. Mouret, "High-efficiency uni-travelling-carrier photomixer at 1.55  $\mu\text{m}$  and spectroscopy application up to 1.4 THz," *Electron. Lett.* **44**(22), 1320–1322 (2008).
28. M. Mikulics M, EA Michael, M. Marso, M. Lepsa, A. van der Hart, H. Luth, A. Dewald, S. Stancek, M. Mozolik, and P. Kordos, "Travelling-wave photomixers fabricated on high energy nitrogen-ion-implanted GaAs," *Appl. Phys. Lett.* **89**, 071103 (2006).

---

## 1. Introduction

Optoelectronic conversion techniques have become the basis of a powerful approach with which the THz frequency gap can be explored. THz Time Domain Spectroscopy is well known and has been extensively used for many years to study various samples. Its popularity is due to its large spectral coverage and the associated coherent detection which allow the refraction and absorption properties to be obtained in the THz spectral band where no versatile tools previously existed. In a similar manner to Fourier transform spectroscopy the resolution is determined by the temporal delay of the probe pulse and is typically limited to values in the region of 1 GHz. With the exception of linear molecules where free induction decay can be observed, THz Time Domain Spectrometers are mainly used to the study of low quality factor resonance phenomena such as those of liquids or solids [1]. When a higher resolution is required the use of optical heterodyning or photomixing is more appropriate. It consists of the conversion of an optical beat into the THz domain by using the non-linearity of an ultrafast photodetector and was first demonstrated by Brown *et al.* in 1995 [2]. Photomixing is now a realistic solution for pure rotational or rovibrational spectroscopy, but up until present it has mainly been confined to the characterization of absorption profiles due to the difficulties encountered when determining the frequency of the THz radiation with sufficient accuracy for high resolution spectroscopy [3–8]. Standard interpolation techniques can be used with one or several absorption lines, this however severely limits the useful tunability of the instrument. Matsuura *et al.* proposed a brilliant solution determining the frequency of previously unobserved transitions of  $\text{NH}_3$  and  $\text{H}_2\text{O}$  [9–11]. Two lasers are locked to different orders of a single Fabry Perot interferometer while the fine tunability is obtained by a third diode phase locked loop to one the two first diode lasers. A similar approach has recently been realized by Abaella *et al.* [12]. In such implementations, the inherent sensitivity of a high finesse Fabry Perot cavity to acoustic noise, thermal drift and refractive index fluctuations require a careful design where different elements are often placed in

vacuum chamber to preserve optical performance and optimise the stability of the THz source. Good beam pointing stabilities are needed to preserve the alignment of laser beams to the fundamental mode of the FP cavity. The calibration and stability of the free spectral range of this high Fabry Perot cavity governs the ultimate frequency accuracy of the spectrometer. Well-known molecular transitions are usually used to measure and calibrate the FSR. Such measurements may be considered to measure wavelength rather than measuring frequency, since such a procedure is used to determine the optical length of the FP cavity [13]. In this paper, we propose to exploit the significant breakthrough in optical metrology measurement by using a frequency comb (FC) obtained from a mode-locked femtosecond laser with a stabilized repetition rate [14,15]. This frequency comb is used like a ruler, to measure or/and to stabilize the difference frequency between two lasers and benefit of the perfect cancellation of any carrier-envelope phase offset that may be present in the original frequency comb. In contrast to Q. Quraishi *et al.*, we propose to use latest developments in the frequency metrology based on femtosecond fiber lasers which form a turnkey system and avoiding the use of expensive and bulky femtosecond Ti:Sa lasers and the associated maintenance [16]. Compactness, power efficiency of such technologies are an attractive proposition to implement a THz synthesizer.

## 2. Experimental configuration and principle of operation

The experimental setup is presented on the Fig. 1. A two-colour continuous wave optical source was composed of a tapered semiconductor amplifier simultaneously seeded by two commercial extended cavity diode lasers (ECDL) nominally operating around 780nm (DL100, TOPTICA Photonics AG). The two-colour beam was divided into two parts; the first was used to generate cw-THz radiation by photomixing while the second was mixed with the frequency comb to synthesize the difference frequency between the ECDL. A standard  $5 \times 5 \mu\text{m}^2$  interdigitated electrode photomixer deposited onto a Low Temperature Grown GaAs semiconductor loaded by a broad band spiral antenna was used to generate the THz radiation. Each  $0.2\mu\text{m}$  width fingers are separated by  $0.8 \mu\text{m}$  as described in ref. 5. The total optical power was in order of 60 mW to produce a DC photocurrent around 1 mA ensuring a microW THz power in the low frequency region of the spectrum and the hundreds of nanoW around 1 THz. The THz radiation produced was propagated through a sample cell before being detected by a composite Si bolometer cooled by liquid He with a loss around 3db compared to the maximum emitted power, allowing a useful dynamic range of around 30dB to be obtained routinely at 1 THz [5]. The optical beat note at the output of the optical amplifier is intensity modulated around 300 Hz by a mechanical chopper allowing a synchronous detection of the emitted THz radiation. A frequency doubled erbium doped modelocked fiber laser (Menlosystems, C-Fiber) provided the FC with a stabilized repetition rate phase-locked onto a synthesizer and can be tuned from 99.790 MHz to 100.200 MHz. Assuming a Gaussian shape, the pulse width of the second harmonic is around 130 fs, associated with a full spectral width of 6 nm large enough to cover several THz. The mean output power of the FC is in order of 90 mW. After mixing with the two-colour beam, it was dispersed by a grating to allow a photodiode to select a small number of FC modes and an ECDL. The beatnote between the ECDL and the nearest FC mode was isolated and phase locked to a local oscillator at 20 MHz, coherently locking the diode to the FC. The locking of the second ECDL to a different FC mode allows the difference frequency between the ECDLs to be synthesised with an accuracy dependent on the FC repetition rate and the local oscillators used in the beatnote phase locked loops. The feedback correction signal produced by a hybrid digital-analog PLL is applied to the ECDL current by a field effect transistor connected directly to the laser diode. The difference of frequency between the diode lasers can be expressed in Eq. (1) as:

$$f_{\text{THz}} = n \cdot f_{rr} \pm f_s \pm f_s \quad (1)$$

where  $n$  is an integer,  $f_{rr}$  is the repetition rate of the femtosecond laser phase locked onto a synthesizer itself referenced onto a low phase noise 10 MHz quartz crystal oscillator (Blue

Top Ultra LowNoise Oscillators from Wenzel).  $f_s$  is the frequency of the synthesizer used to phase lock the beat signals, and the quantity  $(\pm f_s \pm f_s)$  is subsequently named offset frequency. A classical commercial wavemeter is used to remove the ambiguity of the integer. The need to determine the carrier envelope offset (CEO) frequency introduced into the laser cavity has limited the use of FC techniques, however in our case as the ECDL difference frequency is required the measurement of the CEO is avoided.

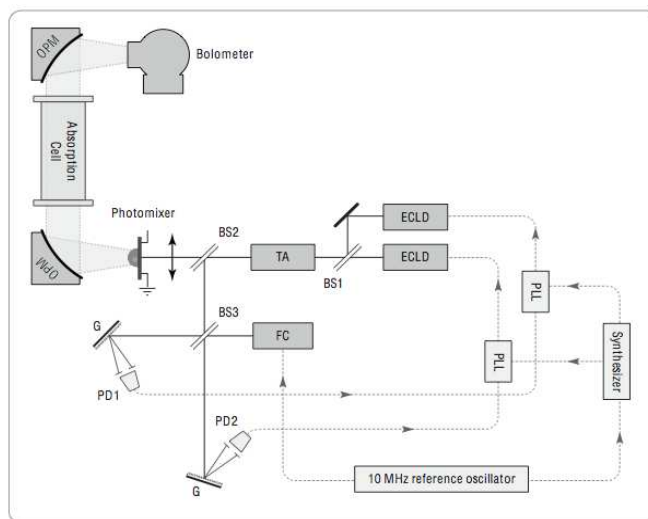


Fig. 1. Experimental setup of the synthesised THz source. A first beam splitter (BS1) is used to overlap the two laser beams from the two External Cavity Diode Laser (ECDL) and seed them to Tapered Amplifier (TA). At the output, optical beat note is divided by a second beam splitter (BS2). A first part is used to produce the THz radiation collected at the backside of the photomixer by a silicon lens. Two Off axis Parabolic Mirrors (OPM) are used to collimate and focus the THz beam through an absorption cell to a cryogenic bolometer. The frequency comb (FC) is overlap with optical beat note by means of a third beam splitter (BS3). Two grating (G) disperse the FC and two lasers to ensure an heterodyne measurement between each ECDL and FC detected by two different photodiodes (PD1- PD2). The heterodyne signals are feed to two Phase Lock Loop (PLL) to synthesized the difference frequency between two ECDL to a synthesizer. A 10 MHz crystal oscillator is used as reference signal for synthesizers, counters and spectrum analyzers required. Solids lines show optical signal, and dashed lines indicate electronic signal.

### 3. Results

#### 3.1 Measurements onto THz synthesizer

The frequency accuracy and the stability of the repetition rate is measured and checked by use of a counter, also referenced to the same 10 MHz reference oscillator. A frequency repetition rate around 100 MHz associated with a standard deviation of  $5 \times 10^{-3}$  Hz for a gate time of 1s and for a measurement time of 18 minutes was routinely obtained. Similar measurements of the two beat notes between ECDL and FC signal typically yielded mean values around 20 MHz associated with standard deviations of 2 Hz. An example of a locked beat note between one of the diode lasers and a FC mode and associated frequency histogram measurement are shown in Fig. 2 and Fig. 3 respectively. The absolute frequency accuracy of the THz synthesizer is then determined by the accuracy of the 10 MHz reference oscillator. In these preliminary experiments, a commercial frequency counter calibrated against Cs etalon is used to check the reference oscillator. The full width of the beat note, shows on Fig. 2, at  $-3$ dB is less than 100 kHz and represents the convolution of the ECDL and FC linewidths which currently exhibit broader optical comb lines than those of Ti:Sa based comb generator [17].

The limited PLL bandwidth, the inherent noise of the fiber based laser system and intrinsic noise of our ECDL current sources may explain the observed spectral purity compared to that Hz level obtained by Q. Quraishi *et al.* [16]. In the present system the PLL bandwidth was estimated to be around 100 kHz. From those measurements we estimate the present useful spectral linewidth of the THz synthesizer better than 200 kHz. This value is well suited to Doppler limited absorption linewidths of small polar molecules, which never exceeds 10 MHz at room temperature. In free running operation, ECDLs exhibit a full width at -3db of around 5 MHz on the timescale of a few seconds, highlighting the efficiency of our PLL.

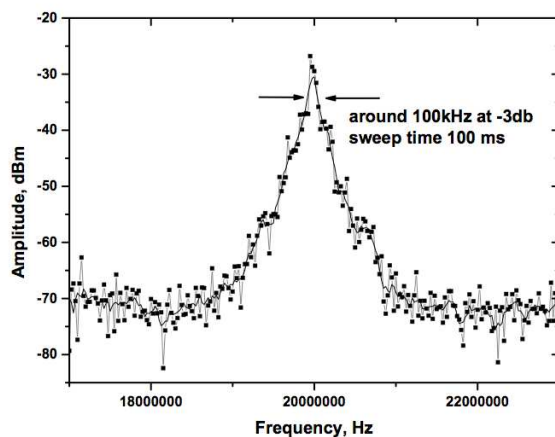


Fig. 2. Phase locked beat note between FC and a ECDL.

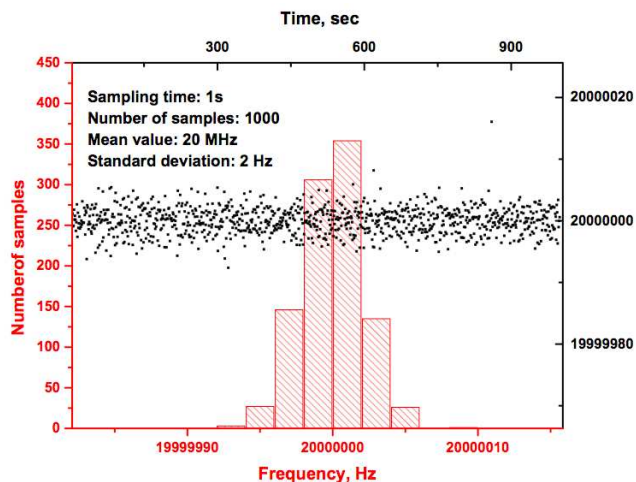


Fig. 3. Histogram of the frequency measurement of the phase locked beat note between FC and a ECDL

### 3.2 spectroscopic measurements

In order to examine the useful accuracy and stability of the synthesized THz frequency a number of spectroscopic measurements of a test molecule are required. In the THz region, Carbonyl Sulfide (OCS) is an ideal candidate as its spectral signature presents a series of intense regularly spaced absorption lines. The  $J + 1 \leftarrow J$  transitions of the most abundant isotopologue have previously been measured with high precision up to 800 GHz ( $J = 66$ ) [18].

The full Doppler width lies between 0.674 MHz and 1.58 MHz at 300 GHz and 1 THz respectively at room temperature. In contrast to Quraishi *et al.* who proposed to tune the THz frequency by scanning the FC repetition rate, the limited gain bandwidth of the ECDL severely restricts the tuning range [16]. Indeed, each laser is locked to a different order of the frequency comb  $n_1$  and  $n_2$ . If the laser repetition rate is scanned, the laser frequencies will also scan according to the corresponding FC mode number. A significantly smaller frequency sweep will be obtained in the synthesised difference frequency governed by  $\Delta n = |n_1 - n_2|$ . In first approximation, the relation between the optical frequency  $f_{opt}$  of pump lasers used in the photomixing process, the THz frequency  $f_{THz}$ , and the related optical tunability  $\Delta f_{opt}$  and THz tunability  $\Delta f_{THz}$  can be written as:

$$\frac{\Delta f_{THz}}{f_{THz}} \approx \frac{\Delta f_{opt}}{f_{opt}} \quad (2)$$

As example, by using Eq. (2), a tunability of 5 MHz at 1 THz requires a repetition rate change of about 500 Hz, corresponding to a ECDL tunability of 1.9 GHz. In order to realize such large frequency excursions the correction signal must be applied to both fast and slow frequency actuators of the ECDL, fast to maintain the phase lock and slow to provide a large tuning range. Here we propose to tune the synthesized frequency by scanning the local oscillator used in the PLL, this has the advantage of requiring a small ECDL frequency excursion so a PLL driving only on the ECDL current FET is easily sufficient. In principle this tuning scheme could allow a continuous tuning range up to  $f_{rr}/2$ , however in practice a single beatnote is isolated by a bandpass filter in the PLL further restricting the tuning range. In our case the maximum continuous tuning range obtained was 11 MHz. Although the continuous tuning range is limited, any THz frequency can be obtained by selection of suitable FC modes and repetition rate. Several examples of the J = 66 absorption line of OCS recorded around 813 GHz are shown in Fig. 4. The full Doppler width of this transition is 1.290 MHz well matched with the actual useful THz linewidth. This absorption line has been recorded by using different repetition rates in order to validate the THz spectrometer. With a difference between the FC modes  $n = 8133$  a repetition rate of 100.001 070 5 MHz corresponded to the line centre frequency, whereas for  $n = 8140$  the repetition rate of 99.915 319 4 MHz was used to synthesise an identical THz frequency. The offset frequency is tuned over 8 MHz to obtain absorption spectra containing 160 points equally spaced at 50 kHz. A time constant of 100 ms was routinely selected for the synchronous detection hence a complete spectra can be recorded in less than one minute. Two different pressures have been used to better distinguish these two different experiments. The absolute frequency is determined by fitting the experimental data using a Gaussian line shape for the Doppler limited broadening in this pressure range. Centre frequency values of  $f_1 = 813\,353.755$  MHz and  $f_2 = 813\,353.763$  MHz for the 2 different repetition rates have been obtained, i.e. a difference of 8 kHz. Firstly, the discrepancy can be neglected compared to the useful linewidth of the THz radiation, thus confirming the validity of the experimental protocol used. Secondly, the two measured values are in good agreement with previous high accuracy measurements  $f_{JPL} = 813\,353.706$  MHz  $\pm 0.060$  MHz tabulated in the Jet Propulsion Laboratory molecular spectroscopy database [19]. The small difference between our measurements and the reference value can be explained by the fact that all our electronics used in this setup are referenced onto a 10 MHz ultra low phase noise crystal oscillator which should be recalibrated on a standard etalon or locked to a GPS signal for the long term accuracy. In any way the actual accuracy is enough to calculate spectroscopic parameters on this molecule, which will be presented on a subsequent part of the present paper. The reproducibility has been tested by repeating the measurement of the absorption line, and results are presented on Fig. 5. A total of 38 recordings were performed on two different days yielding a mean value of 813 353.753 MHz with a standard deviation of 12 kHz. This dispersion can be attributed to the slight variation in some experiment conditions. Once the reference frequency is calibrated, the present THz spectrometer based on frequency comb

should be able to achieve an accuracy better than 50 kHz, limited only by the signal to noise ratio of the transitions recorded. From a practical point of view, the frequency accuracy of the present spectrometer based onto the THz synthesizer will be more affected by the profile of the absorption line, the pressure broadening and base line effects rather than the accuracy of the repetition rate and the offset frequency.

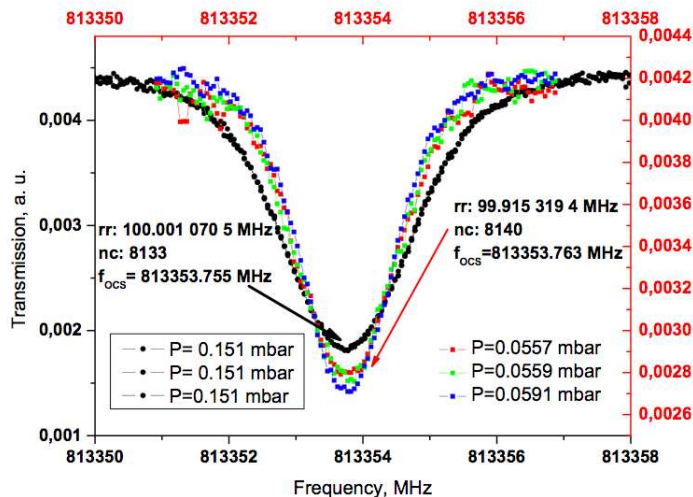


Fig. 4.  $J = 66$  Carbonyl Sulfide absorption line recorded around 813 GHz by using different repetition rate of the THz synthesizer. Two different pressures are used on two different days.

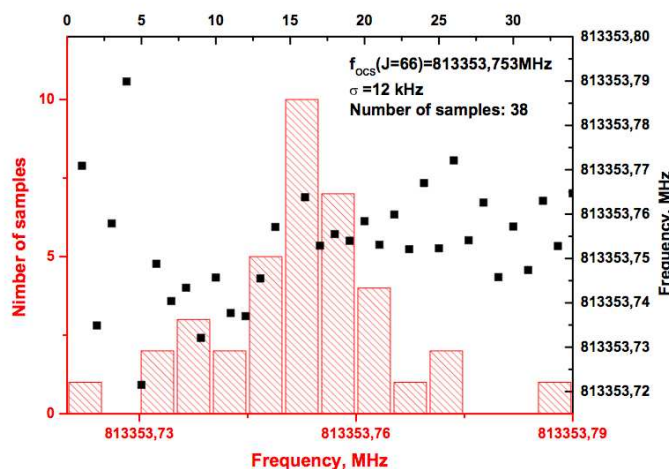


Fig. 5. Reproducibility of the THz spectrometer tested by measuring 38 times the  $J = 66$  transition absorption lines

#### 4. Application to spectroscopy

The capability to probe high  $J$  level rotational transitions of small polar compounds is a principal attraction of high resolution THz spectroscopy. Many spectroscopic databases have only limited measured tabulated data in the THz range for numerous molecules with atmospheric and/or astrophysical interest. Due to the lack of high spectral purity THz

sources, the THz transition frequencies are generally extrapolated from molecular parameters fitted with microwave and submillimeter data. Very often, these extrapolations are unreliable and may lead to false predictions. In the case of the OCS, a global rovibrational analysis has been applied simultaneously by Fayt *et al.* on all data available for the rovibrational energies of the most abundant species  $^{16}\text{O}^{12}\text{C}^{32}\text{S}$  in the electronic ground state [18]. In the ground vibrational state, the rotational constant  $B_0$ , the centrifugal distortion constants  $D_0$  and the sextic constant  $H_0$  have been fitted using the Eq. (3):

$$\nu_{J \rightarrow J+1} = 2B_0(J+1) - 4D_0(J+1)^3 + H_0(J+1)^3 [(J+2)^3 - J^3] \quad (3)$$

where  $\nu_{J \rightarrow J+1}$  is the frequency of the  $J \rightarrow J + 1$  transition. In the global fit of Fayt *et al.*, 49 measured frequencies from microwave and submillimeter experiments have been retained [18]. The majority of these frequencies are listed in the JPL spectroscopic database and have been determined with an experimental uncertainty better than 60 kHz [19]. Above 700 GHz, only four  $J \rightarrow J + 1$  transitions (57 $\rightarrow$ 58, 58 $\rightarrow$ 59, 65 $\rightarrow$ 66, 66 $\rightarrow$ 67) measured by Helminger *et al.* were included [20]. More recently, Golubiatnikov *et al.* performed very accurate frequency measurements of  $^{16}\text{O}^{12}\text{C}^{32}\text{S}$  rotational lines using the Lamb-dip absorption technique with the submillimeter spectrometers of Kiel and Nizhni Novgorod [21]. 26  $J \rightarrow J + 1$   $^{16}\text{O}^{12}\text{C}^{32}\text{S}$  transition frequencies, up to 490 GHz, have been measured with an accuracy of about one kHz and 12 other frequencies transitions ( $73 \leq J \leq 78$  and  $84 \leq J \leq 89$ ) have been measured in the THz domain with an accuracy  $\leq 30$  kHz. Aiming to compare the performance of the cw-THz spectrometer with these previous measurements, 31 rotational lines of  $^{16}\text{O}^{12}\text{C}^{32}\text{S}$  have been measured in this study and are listed in Table 1. The rotational lines corresponding to  $J \rightarrow J + 1$  transitions with  $65 < J < 106$  were recorded in the 0.8 – 1.2 THz frequency range. For each transition, many recordings have been measured under different conditions and used to determine the mean transition frequency and its standard deviation, see Table 1. Using the SPFIT program, the molecular constants  $B_0$ ,  $D_0$  and  $H_0$  have been fitted with these new THz measurements using the Eq. (3) [22]. This program applies a weighted least-squares minimisation procedure to the measured frequencies using standard statistical treatment [23]. The experimental errors listed in Table 1 were used as statistical weight and two values have been chosen: 100 kHz for  $\nu < 1.1$  THz and 200 kHz for  $\nu > 1.1$  THz in order to reduce the level of confidence of measurements at high frequency which display a lower SNR. The uncertainties listed in Table 2 are calculated as part of the minimisation routine and are dependent on the overall quality of the fit. Four sets of molecular constants are compared: the first set is from the microwave and submillimeter measurements used in the global fit of Fayt *et al.*, the second set was obtained with the Lamb-dip measurements of Golubiatnikov *et al.*, the third set is deduced from the frequencies measured in this study and listed in Table 1, finally the fourth set was obtained associating the Lamb-dip measurements below 800 GHz and the cw-THz measurements of the Table 1 [18,21]. The comparison between the molecular parameters fitted with the cw-THz measurements and the first set of data shows that the THz measurements did not degrade the uncertainty of the rotational constant  $B_0$  fitted with the microwave and millimeter data but they really improved the accuracy of the centrifugal distortion constants. In particular, the new THz measurements allowed the sextic constant  $H_0$  to be determined with a relative uncertainty of 1.5% compared to the 8.3% for the first set. This comparison demonstrates that the measured frequencies with the THz photomixing synthesizer based on a fiber frequency comb is very efficient to improve the molecular parameters implied in the high order terms of the rotational lines. In the Table 1, the differences between the measured frequencies and the calculated frequencies from the fitted constants of the Table 2 are detailed. A Root-Mean-Square (RMS) less than 100 kHz, deduced from the 32 frequencies measured, demonstrates that the THz photomixing synthesizer is competitive with microwave and submillimeter techniques. More surprisingly, the performance of cw-THz synthesizer is comparable to that obtained with the Lamb-dip absorption technique which is very well known for its high accuracy frequency measurement

of rotational transitions. The standard deviations listed in Table 1 are comparable as those determined in ref [21]. for the  $J \rightarrow J + 1$  transitions, commonly measured in the two studies. Moreover, in the Table 2, the comparison between the second and the fourth set of fitted parameters shows that the degree of accuracy of the fitted OCS molecular constants are relatively close.

**Table 1. Frequencies of the  $^{16}\text{O}^{12}\text{C}^{32}\text{S}$  rotational lines measured in this work by using the THz photomixing spectrometer and calculated with the fitted molecular constants of the Table 2.**

Transition $J \rightarrow J + 1$	cw-THz Frequency (MHz)	Standard Deviation (kHz) <sup>a</sup>	Error (kHz) <sup>b</sup>	Obs-Calc. (kHz) <sup>c</sup>
66→67	813353.7325	6.5	100	89.32
67→68	825445.4917	7.9	100	70.86
68→69	837535.1200	35.7	100	48.55
69→70	849622.5985	25.1	100	34.86
70→71	861707.8677	12.4	100	1.68
71→72	873790.9031	7.7	100	-44.10
72→73	885871.6333	23	100	-142.50*
73→74	897950.3235	6.3	100	30.70
74→75	910026.5950	13.7	100	45.33
75→76	922100.3153	11.8	100	-116.84*
76→77	934171.7659	8.8	100	-180.52*
77→78	946240.9481	39.0	100	-83.00
78→79	958307.5968	6.4	100	-88.97
79→80	970371.8792	10.8	100	13.21
80→81	982433.5251	14.8	100	-18.25
81→82	994492.6586	11.7	100	-26.81
82→83	1006549.2890	12.4	100	28.27
83→84	1018603.4830	15.6	100	245.13*
84→85	1030654.6130	10.1	100	27.61
85→86	1042703.2700	99.0	100	-1.83
86→87	1054749.2610	27.6	100	-4.74
87→88	1066792.6310	64.3	100	95.35
88→89	1078833.1820	28.4	100	131.91*
89→90	1090870.7840	46.0	100	6.4
92→93	1126966.7090	35.0	200	-214.56*
93→94	1138993.2320	30.9	200	43.44
97→98	1187068.5260	35.5	200	36.85
98→99	1199079.6780	35.5	200	-38.97
102→103	1247093.1600	33.7	200	-132.96
103→104	1259088.6500	181.0	200	-45.41
104→105	1271080.8630	132.5	200	24.87
105→106	1283069.5340	116.3	200	-155.54

<sup>a</sup> Standard deviation obtained after averaging of many line records at different conditions.

<sup>b</sup> Estimation of the experimental error used as weight in the fitting procedure.

<sup>c</sup> "Obs - Calc." is the difference between the measured frequencies and the calculated frequencies from the fitted molecular parameters (Table 2). \* when difference is superior to the estimated experimental error

**Table 2. Rotational and centrifugal distortion constants of  $^{16}\text{O}^{12}\text{C}^{32}\text{S}$  fitted by different sets of frequencies. Uncertainties given in parentheses are in units of the last digit quoted.**

	Global fit <sup>a</sup>	Lamb-dip measurements <sup>b</sup>	cw-THz measurements <sup>c</sup>	Cw-THz + millimeter measurements <sup>d</sup>
$B_0$ (MHz)	6081.4921205 (99)	6081.4921150 (52)	6081.4921160 (99)	6081.4921049 (94)
$D_0$ (kHz)	1.3014448 (271)	1.3014274 (32)	1.3013639 (148)	1.3014316 (89)
$H_0$ (mHz)	-0.08320 (690)	-0.08938 (33)	-0.08541 (126)	-0.08022 (98)
N*	47	61	32	72
R.M.S.** (kHz)	16.985	30.824	94.664	73.495

<sup>a</sup> Global fit of Fayt *et al.* including J→J + 1 transitions with J<61 for the ground vibrational state [18]

<sup>b</sup> Fit detailed in ref [21], including lamp-dip measurements of J→J + 1 transitions in the millimeter (15<J<40) and in the THz (72<J<90) spectral regions.

<sup>c</sup> Fit performed in this work with measured frequencies listed in Table 1.

<sup>d</sup> Fit including lamp-dip frequency measurements [21] up to 800 GHz and the cw-THz measurements listed in Table 1

\* Number of fitted lines

\*\* Microwave Root Mean Square defined in the SPFIT program [22]

## 5. Conclusions

The photomixing technique associated to new developments in optical metrology based on the fiber frequency comb is now a powerful solution to effectively cover a large part of the THz frequency gap. Relatively good linewidth, large bandwidth associated with a versatile means of high accuracy frequency measurement are relevant requirements of such optoelectronic conversion. THz radiation can be produced with a 10 MHz tuning range around any desired frequency. Spectroscopic measurements of OCS have been performed and compared to high accuracy Doppler free data confirming the consistence of the present spectrometer based on a THz synthesizer. Despite that useful frequency accuracy is more affected by the line profile than absolute accuracy of arrangement, we plan to lock our reference crystal oscillator onto a well controlled GPS signal to avoid any systematic error in future studies. The good reproducibility observed in the preliminary spectroscopic experiments should also improve the sensitivity of the THz spectrometer for trace gas detection [24,25]. Indeed, frequency instabilities are often a tedious problem to normalize absorption spectra due to large fluctuations in the base line, and so prevent the measurement of small transitions. While studies under 1 THz can benefit to formidable progress in the harmonics generation, developed for astronomy purpose, since the different elements are now commercially available up to 800 GHz, explorations above one THz are still hampered by the lack of coherent sources. So photomixing technique has strong potential in the high part of the frequency gap since some demonstrations has been reported up to 3.2 THz [3]. Although many solutions can be applied to improve specifications of a classical photomixing spectrometer from the point of view of the optical part, the maximum output power is still limited in the nW range around 1.5 THz and so hamper its use outside the laboratory. Future progress in the photomixer to push up the emitted power will govern the viability of this technique. On this point some progress are expected mainly by use of new UniTravellingCarrier (UTC) photodiodes which working at telecom wavelength and so open new possibilities to develop fiber based portable instrument [26,27]. Distributed photomixer using large area of semiconductor to prevent thermal failure is also a possible alternative to increase the THz emitted power [28].

## Acknowledgements

This work was partially funded by Agence De l'Environnement et de la Maîtrise de l'Energie (ADEME), the region of Nord Pas-de-Calais, the European Commission, and the Délégation Générale pour l'Armement (projet de Recherche Exploratoire et Innovation n°06.34.037). The Laboratoire de Physico-Chimie de l'Atmosphère and the Laboratoire de Physique des Lasers, Atomes et Molécules participate in the Centre d'Etudes et de Recherches Lasers et Applications (CERLA).